Semicond. Sci. Technol. **27** (2012) 074002 (13pp) doi:10.1088/0268-1242/27/7/074002

# Atomic layer deposition for photovoltaics: applications and prospects for solar cell manufacturing

**J A van Delft, D Garcia-Alonso and W M M Kessels**

Department of Applied Physics, Eindhoven University of Technology, PO Box 513, 5600 MB Eindhoven, The Netherlands

E-mail: w.m.m.kessels@tue.nl

Received 6 January 2012, in final form 9 January 2012
Published 22 June 2012
Online at stacks.iop.org/SST/27/074002

**Abstract**

Atomic layer deposition (ALD) is a vapour-phase deposition technique capable of depositing high quality, uniform and conformal thin films at relatively low temperatures. These outstanding properties can be employed to face processing challenges for various types of next-generation solar cells; hence, ALD for photovoltaics (PV) has attracted great interest in academic and industrial research in recent years. In this review, the recent progress of ALD layers applied to various solar cell concepts and their future prospects are discussed. Crystalline silicon (c-Si), copper indium gallium selenide (CIGS) and dye-sensitized solar cells (DSSCs) benefit from the application of ALD surface passivation layers, buffer layers and barrier layers, respectively. ALD films are also excellent moisture permeation barriers that have been successfully used to encapsulate flexible CIGS and organic photovoltaic (OPV) cells. Furthermore, some emerging applications of the ALD method in solar cell research are reviewed. The potential of ALD for solar cells manufacturing is discussed, and the current status of high-throughput ALD equipment development is presented. ALD is on the verge of being introduced in the PV industry and it is expected that it will be part of the standard solar cell manufacturing equipment in the near future.

(Some figures may appear in colour only in the online journal)

## 1. Introduction

Interface engineering is of vital interest for solar cell manufacturing as the properties of interfaces between different materials play a decisive role in the performance of photovoltaic (PV) devices. Atomic layer deposition (ALD) is a vapour-phase deposition technique that can be used to tailor interface properties by depositing high-quality thin films with precise growth control, very good uniformity over large areas and excellent step coverage on non-planar surfaces [1–3]. These unique features make ALD very attractive for many solar cell designs that require (ultra)thin layers.

The virtue of the ALD method is that the deposition is controlled at the atomic level by self-limiting half-reactions. During the so-called ALD cycle, the substrate is sequentially exposed to different gas-phase precursors and reactants resulting typically in film growth of one sub-monolayer per cycle. To guarantee self-limiting growth dictated by the surface chemistry, each precursor and reactant step is followed by an inert-gas purge step to prevent chemical vapour deposition (CVD)-like reactions to occur. Other benefits of the ALD method are the relatively low substrate temperature used in the process, typically 150–350 °C, the fact that ALD can readily produce multilayer structures and nanolaminates, and its capability to grow dense films with a low pinhole density.

The use of ALD for several PV applications has been researched from the early 1990s to the present day. The first application was reported by the group of Bedair and co-workers in 1994. This ALD research, known as 'atomic layer epitaxy' (ALE) at that time, was on GaAs, AlGaAs and AlAs films used as absorbers in multijunction solar cells [4, 5]. Reports on the application of ZnSe buffer layers for CIGS solar cells [6], and boron-doped ZnO films as transparent conductive oxide (TCO) deposited by ALD followed shortly afterwards

 

**Table 1.** Overview of solar cell technologies in which ALD materials have been applied (status February 15, 2012).

| Solar cell type | Application | Thickness (nm) | ALD materials | References |
|---|---|---|---|---|
| AlGaAs/GaAs multijunction | Absorber | 30–400 | GaAs | [4, 5] |
| | | | AlGaAs | [4, 5] |
| | | | AlAs | [4] |
| *a*-Si:H | Transparent conductive oxide | 400 | ZnO:B | [7, 8] |
| c-Si | Surface passivation layer | 5–30 | $Al_2O_3$ | [10–31] |
| CIGS | Buffer layer | 10–70 | ZnSe | [6] |
| | | | (Zn,Mg)O | [32–38] |
| | | | Zn(O,S) | [32, 33, 35, 39–44] |
| | | | $In_2S_3$ | [39, 43, 45–51] |
| | | | GaS | [39] |
| | | | ZnS | [39] |
| | | | $Al_2O_3$ | [43] |
| | | | $TiO_2$ | [43] |
| | | | ZnO | [52–56] |
| | | | Zn-Sn-O | [57, 58] |
| | Diffusion barrier layer | 100–300 | $Al_2O_3$ | [59] |
| | Encapsulation layer | 10–55 | $Al_2O_3$ | [60, 61] |
| CdTe | Window layer/*n*-type layer | ∼100 | Zn(O,S) | [62] |
| Organic | Encapsulation layer | 15–200 | $Al_2O_3$ | [63, 64] |
| | | | $Al_2O_3$ / $HfO_2$ | [65, 66] |
| | Electron selective layer | 1–35 | $Al_2O_3$ | [67] |
| | | | ZnO | [68, 69] |
| | | | $TiO_2$ | [70, 71] |
| | Transparent conductive oxide | 150 | ZnO:Al | [72] |
| Dye-sensitized | Barrier layer | 0.1–25 | $Al_2O_3$ | [73–82] |
| | | | $TiO_2$ | [73, 83, 84] |
| | | | $HfO_2$ | [80] |
| | | | $ZrO_2$ | [85] |
| | Photoanode | 5–90 | $TiO_2$ | [84, 86–88] |
| | | | ZnO:Al | [84] |
| | | | $SnO_2$ | [84] |
| | | | ZnO | [89–91] |
| | | | $TiO_2$:Ta | [92] |
| | Blocking layer | 7–20 | $SnO_2$ | [81] |
| | | | $TiO_2$ | [74, 77, 92] |
| | Compact layer | | $HfO_2$ | [93] |
| | Transparent conductive oxide | 7 | $In_2O_3$:Sn | [87] |
| | Sensitizer | 5 | $In_2S_3$ | [94] |
| Heterojunction nanostructured | Absorber | –[a] | $Cu_xS$ | [95] |
| | | | $CuInS_2$ | [96–100] |

[a] $Cu_xS$ or $CuInS_2$ are infiltrated into $TiO_2$ pores, no exact thickness is specified.

[7, 8]. Especially in the last few years, significant developments have been made in academic research on ALD and its application into the PV industry. This increased popularity is manifested by the growing number of publications and the large set of thin-film materials and applications that have been studied for solar cells (see table 1). PV applications include absorber films, buffer layers, interface layers, transparent front contacts, photoanodes, encapsulation layers and surface passivation films.

In this article, some of the most successful applications of ALD films in PV research are reviewed and recent developments are introduced. The intention, however, is not to give an in-depth review of all materials researched for PV applications (for this, see Bakke *et al* [9]). The intention is to focus on results obtained with actual solar cells with at least one layer deposited by ALD and to address the viability of this technique for the PV industry. An important requirement for the latter is that the ALD process should be low cost and time efficient compared to established technologies, and should lead to better solar cell performances compared to commonly used approaches. The relevance of the ALD method for crystalline silicon (c-Si) solar cells, copper indium gallium selenide (CIGS) solar cells, organic photovoltaic (OPV) solar cells, dye-sensitized solar cells (DSSC) and several nanostructured solar cell concepts (see figure 1) is presented in the following sections. Furthermore, advances made in the commercialization of high-throughput ALD equipment for the PV industry are discussed.

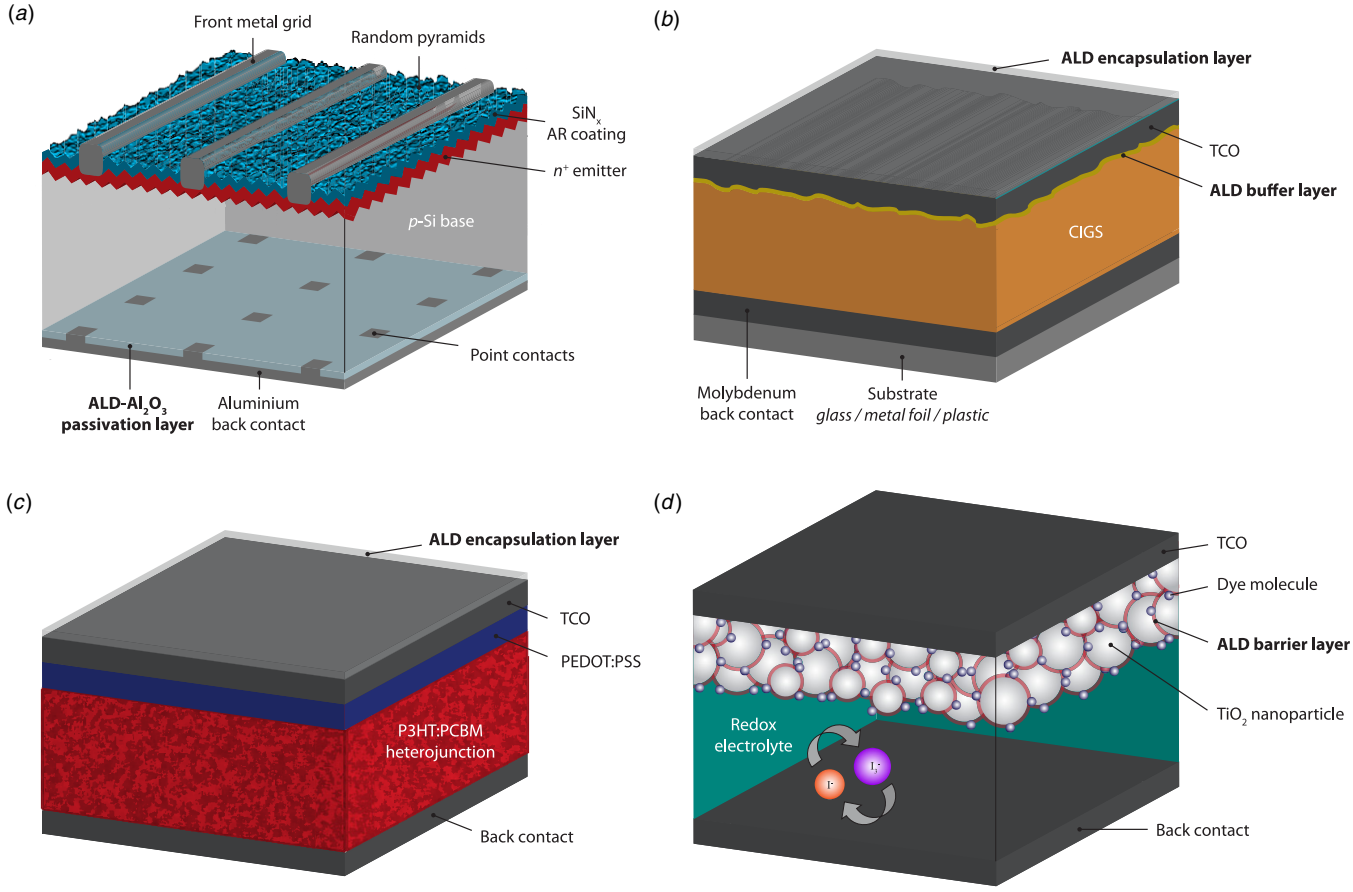


**Figure 1.** Thin films deposited by ALD for various solar cell concepts: (*a*) surface passivation layer for c-Si solar cells; (*b*) encapsulation and Cd-free buffer layer for CIGS solar cells; (*c*) encapsulation of flexible OPV cells; (*d*) barrier layer for DSSCs.

## 2. Surface passivation layers for c-Si solar cells

In the c-Si solar cell industry there is a very strong focus on the reduction of the cost per watt peak. Reducing the cell thickness and improving its efficiency are logical strategies to achieve this goal. For both approaches, it is of vital importance to reduce the electronic losses at the c-Si interfaces, which can be achieved by effective surface passivation layers. Depending on the cell design, these passivation layers can be applied to the front and/or back side of the Si solar cell.

In conventional c-Si solar cells, a screen-printed aluminium metallization is applied to the rear side leading to a back-surface-field (BSF) in the contact firing process. This Al-BSF reduces the recombination of minority charge carriers at the rear side. Although this process is widely applied in the PV industry, it is not suitable for future generation cells with thicknesses below 150 $\mu$m. For such thin wafers, the application of an Al-BSF results in unacceptable wafer bowing and high recombination losses [101]. Therefore, the PV industry is searching for alternatives to replace the Al-BSF by a dielectrically passivated rear. Besides improving the electrical quality (i.e. passivation properties), dielectric surface passivation layers can also contribute to reduce optical losses (i.e. increased internal reflection) at the rear of the cells. $Al_2O_3$ is considered as one of the most promising surface passivation materials.

In 2006 Agostinelli *et al* and Hoex *et al* showed that $Al_2O_3$ films deposited by ALD yield an excellent level of surface passivation on both low-resistivity *n*- and *p*-type Si [102, 103]. In subsequent research, the excellent passivation quality of $Al_2O_3$ was attributed to a combination of chemical passivation—i.e. reduction of the defect density at the interface—and field-effect passivation by the presence of a high fixed negative charge density ($\sim 10^{12}$–$10^{13}$ cm$^{-2}$) at the $Al_2O_3$-Si interface. $Al_2O_3$ deposited by ALD from $Al(CH_3)_3$ precursor is a well-understood process whose main benefits are the wide range of deposition temperature (150–250 °C) and the freedom of choice of oxidant ($O_2$-plasma, $O_3$ or $H_2O$). All these process conditions result in good passivation layers after annealing at 400 °C [104, 105]. The high level of surface passivation, as indicated by the lifetime of the minority carriers, is maintained for ultrathin films down to a thickness of ~5 and ~10 nm for the $O_2$-plasma- and $H_2O$-based ALD processes, respectively (see figure 2) [106].

The suitability of a passivation layer for implementation in solar cells depends on factors such as the thermal, UV, and long-term stability, the optical properties (e.g. refractive index and extinction coefficient) and the processing requirements (e.g. deposition temperature). The thermal stability is important when the passivation layers are applied in the conventional manufacturing process flows and in these cases the application of additional capping layers of materials such as $SiO_2$ or *a*-$SiN_x$:H can be beneficial. The stability against

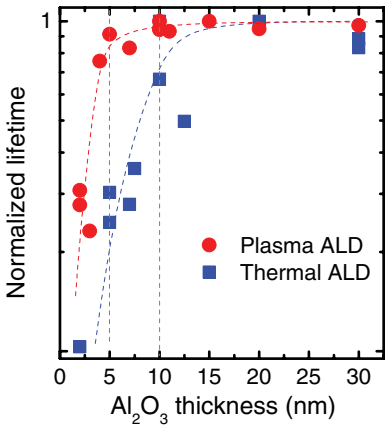


**Figure 2.** Normalized lifetime of the minority carriers in c-Si at an injection level of $\Delta n = 10^{15}$ cm$^{-3}$ as a function of the thickness of $Al_2O_3$ prepared by plasma ALD ($O_2$-plasma) and thermal ALD ($H_2O$). The lifetime is normalized by the highest effective lifetime measured. (Reprinted from [106] with permission from John Wiley & Sons, Ltd.)

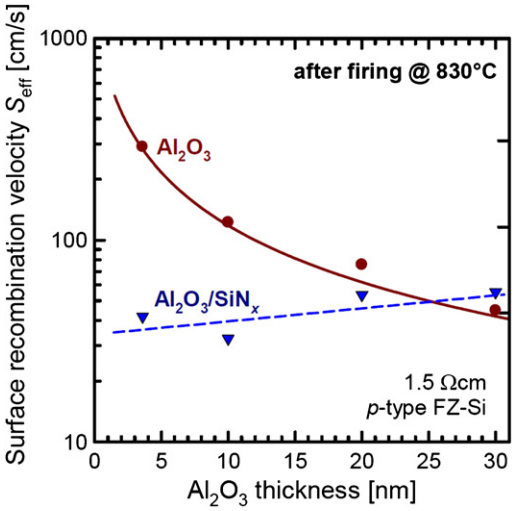


**Figure 3.** Effective surface recombination velocity for *p*-type Si measured at an injection level of $\Delta n = 10^{15}$ cm$^{-3}$ after firing at 830 °C as a function of the $Al_2O_3$ layer thickness for (i) a single layer $Al_2O_3$ deposited by plasma ALD and (ii) a stack of $Al_2O_3$ and PECVD-*a*-$SiN_x$:H (75 nm thick) (© 2010 IEEE. Reprinted, with permission, from [20]).

high temperature (>800 °C) contact firing processes has been investigated for ALD-$Al_2O_3$ passivation layers and stacks of ALD-$Al_2O_3$/PECVD-$SiN_x$ and ALD-$Al_2O_3$/PECVD-$SiO_2$ by several authors [10, 107–110]. Figure 3 shows the effective surface recombination velocity $S_{\text{eff}}$—a measure for the level of surface passivation—as a function of the ALD-$Al_2O_3$ layer thickness for different layer configurations (ALD-$Al_2O_3$ single layer and ALD-$Al_2O_3$/PECVD-$SiN_x$ stack). The $S_{\text{eff}}$ values after the high temperature process are higher than the initial values (not shown; usually <10 cm s$^{-1}$ [111]), however, the remaining level of passivation is by far sufficient for the implementation of these layers into industrial-type silicon solar cells.

The first application of ALD-$Al_2O_3$ for actual solar cells was reported for *p*-type PERC (passivated emitter and rear cell) solar cells [11]. Schmidt *et al* from ISFH used plasma-enhanced ALD-$Al_2O_3$ to passivate the rear surface, as a single layer and as a stack combined with PECVD-$SiO_2$. The best cell efficiency in this report was 20.6% (using the stack configuration) which was slightly higher (0.1% absolute) than the reference cell with thermally grown $SiO_2$. In later works, efficiencies up to 21.4% were obtained for similar solar cells [12, 13]. No separate annealing step was necessary to activate the surface passivation since the thermal budget during the solar cell manufacturing process proved to be sufficient to obtain excellent surface passivation. Moreover, the solar cells did not suffer from the so-called parasitic shunting effect typically observed for *p*-type c-Si solar cells passivated by dielectrics with a high positive charge density such as *a*-$SiN_x$:H. The high fixed negative charge density in the $Al_2O_3$ induces an accumulation layer rather than an inversion layer in the c-Si underneath the rear surface.

The presence of a high negative charge density makes $Al_2O_3$ also an ideal candidate for the passivation of highly doped *p*-type silicon. Hoex *et al* demonstrated experimentally that $Al_2O_3$ films yielded a lower surface recombination velocity on highly doped *p*-type silicon than thermal $SiO_2$, as-deposited *a*-$SiN_x$:H and *a*-Si:H films [112, 113]. This is highly relevant for *n*-type Si solar cells with boron-diffused $p^+$-type emitters that have an enormous economical potential but whose passivation was found to be very challenging [114]. High surface passivation performance at the device level has also been confirmed by a large increase in energy conversion efficiency obtained for *n*-type c-Si PERL (passivated emitter with rear locally diffused) solar cells prepared by Fraunhofer ISE. In this case, the front side B emitter (sheet resistance of 140 Ω sq$^{-1}$) was passivated by a stack consisting of a 30 nm thick ALD-$Al_2O_3$ film and a 40 nm thick PECVD-*a*-$SiN_x$:H film resulting in, at that time, a record efficiency of 23.2% [14]. Other solar cell results have been reported since then by research groups at ITRI [15], ECN [16], the University of Konstanz [17], INES [18] and Imec [19].

Besides the presence of a high fixed negative charge density, other benefits of depositing $Al_2O_3$ by ALD are the absence of absorption in the visible part of the spectrum (band gap amorphous $Al_2O_3$ is ∼6.4 eV [111]), the low processing temperature (avoiding bulk lifetime degradation of c-Si), and the excellent uniformity on large area substrates.

## 3. Buffer layers for CI(G)S solar cells

Chalcopyrite thin-film solar cells based on $Cu(In,Ga)Se_2$ (CIGS) and related absorbers such as $CuInS_2$ (CIS) and $Cu(In,Ga)(S,Se)_2$ (CIGSSe) commonly use CdS buffer layers. Such a buffer layer, typically 10–70 nm thick, is required to ensure good interfacial properties between the CIGS absorber and the (undoped) ZnO window layer. The absence of a buffer layer results in a low open circuit voltage ($V_{\text{oc}}$) and poor efficiency, amongst others, due to the large negative conduction band offset (CBO) at the CIGS/ZnO interface [36].

One of the objectives in current research is to find a substitute for CdS as there are intrinsic material limitations

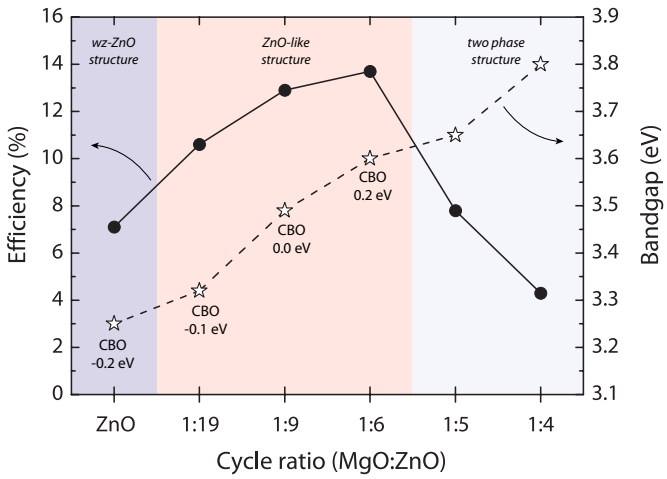


**Figure 4.** CIGS cell efficiency and band gap of (Zn,Mg)O buffer layers deposited by ALD at 120 °C as a function of the MgO:ZnO cycle ratio. The conduction band offset (CBO) and the crystal structure is indicated in the figure (wz stands for wurtzite). Note that the horizontal axis is not to scale. (Data from reference [36].)

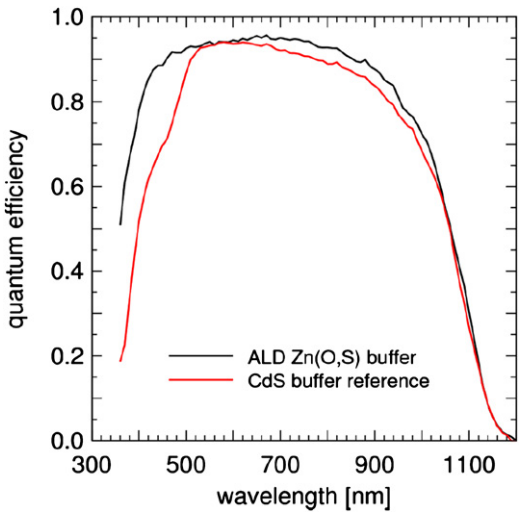


**Figure 5.** External quantum efficiency of a coevaporated CIGS solar cell with an ALD-Zn(O,S) buffer layer. Data for a cell with a chemical bath deposited CdS buffer layer are shown as reference. (Reprinted from [44] with permission from WIP-Renewable Energies.)

and industrial processing drawbacks. The low band gap of CdS (2.4–2.5 eV) for example, limits the solar cell performance due to absorption losses in the short wavelength range, resulting in a reduced short circuit current density $J_{sc}$. From the industrial processing point of view, the chemical bath deposition (CBD) method that is used as a standard technique to deposit CdS layers is not desirable since it is the only liquid-phase deposition step in the CIGS solar cell manufacturing process. Furthermore, Cd is classified as toxic, hazardous and carcinogenic [115]. Therefore, it is preferable to use alternative materials and methods to produce the buffer layers.

Following the initial study of Ohtake *et al* published in 1995 [6], ALD of a wide variety of Cd-free materials (oxides, sulfides and selenides) for the application in CIGS solar cells has been investigated by a considerable number of research groups (see table 1). ALD provides excellent control over the film composition and thereby excellent control over the band gap and CBO. Moreover, ALD is a dry process that can be easily integrated alongside the other vacuum deposition steps in the production process, minimizing the exposure of the cells to atmospheric conditions. Extensive reviews of (ALD) buffer layers have been published by Naghavi *et al* and Bakke *et al* [9, 116, 117]. (Zn,Mg)O, Zn(O,S) and $In_2S_3$ have been identified as the most promising Cd-free ALD materials.

ALD-prepared (Zn,Mg)O buffer layers can be deposited by alternating ZnO and MgO ALD cycles using $Zn(C_2H_5)_2$ and $MgCp_2$ precursors and $H_2O$ as the oxidant source. The self-limiting growth characteristic of ALD allows for layer-by-layer doping of the ZnO films by Mg, where the doping concentration is determined by the ratio between the ZnO and MgO cycles. As shown in figure 4, the band gap of the (Zn,Mg)O films increases from 3.3 eV towards 3.8 eV with increasing amount of Mg in the ZnO structure until phase segregation occurs [36, 37]. The addition of Mg increases the resistivity and also the conduction band of ZnO, resulting in an improved band alignment with the CIGS absorber and thus a better device efficiency [116, 118]. The ALD temperature window for good-quality buffer layers is narrow (105–135 °C) and the best (Zn,Mg)O buffer layers with a band gap of about 3.6 eV were deposited at 120 °C. For films deposited at higher temperatures, a significant drop in device efficiency was observed due to lower open circuit voltage $V_{oc}$ and fill factor *FF* values possibly due to deterioration of the interface quality. Coevaporated CIGS cells with a 150 nm thick ALD-prepared (Zn,Mg)O buffer layer yielded efficiencies up to 18.1% [32]. The absorption of these cells in the blue wavelength range is much better than that of the reference cells (using CdS buffer layers), resulting in an increased $J_{sc}$ and efficiency.

Zn(O,S) buffer layers also benefit from the ability of ALD to control the film composition from pure ZnO to pure ZnS by changing the ratio between the $Zn(C_2H_5)_2$ precursor and the two reactants $H_2O$ and $H_2S$. The solar cell performance depends strongly on the composition of the Zn(O,S) buffer layer. On the one hand, buffer layers need to be ultrathin when the sulfur content is too high to prevent blocking of the photocurrent. On the other hand, a drop in $V_{oc}$ occurs if the sulfur content is too low. Both phenomena can be explained by the CBO at the CIGS/Zn(O,S) interface which is discussed in detail by Plater-Björkman *et al* [42]. The best Zn(O,S) buffer layer had an intermediate sulfur concentration and was obtained by the deposition of 70 ALD cycles of Zn(O,S) at 120 °C, where in every seventh cycle $H_2S$ instead of $H_2O$ was used as the reactant. The application of these 25 nm thick Zn(O,S) buffer layers to 12.5 × 12.5 $cm^2$ coevaporated CIGS solar cells led to efficiencies up to 18.5% [44]. Similar to the CIGS cells with an ALD-prepared (Zn,Mg)O buffer layer, these cells have an increased absorption in the blue wavelength range compared to CdS reference cells (see figure 5). Additionally, the quantum efficiency between 600 nm and 1000 nm increased, which was attributed to a wider space charge region in the cells leading to an improved carrier collection for long wavelengths. Mini-modules (16 series interconnected cells; cell width of 5 mm) with

Zn(O,S) buffer layers showed both a higher $V_{oc}$ and higher $J_{sc}$ than the CdS-reference modules. The best efficiency obtained was 14.8%, which was more than 1% absolute higher than the CdS-reference module [44].

ALD-$In_2S_3$ buffer layers are usually deposited using $In(acac)_3$ as precursor and $H_2S$ as reactant. In this particular case, the deposition temperature is a crucial parameter. Compared to the ALD process of (Zn,Mg)O and Zn(O,S), relatively high temperatures are used, typically 200–210 °C. At these temperatures small amounts of Cu, Ga and In from the CIGS absorber diffuse into the $In_2S_3$ films during the deposition [45]. This effect promotes the formation of the *p–n* junction due to an inversion of the near-interface region of CIGS from *p*-type to *n*-type. At temperatures above 210 °C, an undesired intermediate phase is formed between CIGS and $In_2S_3$ which deteriorates the cell performance. The highest cell efficiencies have been obtained for cells with thin $In_2S_3$ buffer layers of 30–40 nm deposited by ALD [51], with 16.4% as the best efficiency [47]. This process has been scaled up successfully to 30 × 30 $cm^2$ module areas, leading to module efficiencies of 12.9% which is comparable to the CdS-reference module [49]. In the blue wavelength region between 380 nm and 600 nm, the quantum efficiency of the devices with $In_2S_3$ buffer layers is higher than the Cd-containing reference device due to the higher band gap of $In_2S_3$ (2.7 eV). Above all, the main benefit of using $In_2S_3$ buffer layers is that the cell does not suffer from the light soaking effect which has been observed for CIGS devices with other alternative Cd-free buffer layers [50].

## 4. Encapsulation of CIGS and OPV solar cells

The encapsulation of flexible CIGS and OPV cells is required to protect them against moisture and oxygen from the ambient. Traditionally, glass is used as encapsulating material for many solar cells because of its negligible water vapour transmission rate. However, robust, transparent and flexible materials are required in the case of flexible CIGS and OPV cells. The capability to deposit virtually pinhole-free inorganic films at low temperature renders ALD a good candidate technique for this application [60, 61, 63–65].

Carcia *et al* demonstrated that an encapsulation layer of 55 nm $Al_2O_3$ deposited by ALD on top of a CIGS cell provides excellent moisture permeation protection [61]. As shown in figure 6, the level of protection was found similar to that of glass. The $V_{oc}$ and *FF* values did not decrease significantly under accelerated ageing testing conditions (85 °C/85% relative humidity) which demonstrates the superb encapsulation quality of $Al_2O_3$. Furthermore, the deposition of the $Al_2O_3$ at 120 °C also worked as an annealing step, which improved the initial efficiency of the ALD-coated CIGS cell from 11.5% to 13.1%.

Also, nanolaminated ALD films can be used to encapsulate flexible PV devices. OPV cells, which have a great commercial potential due to low costs of materials and processing, have been successfully encapsulated by $Al_2O_3/HfO_2$ nanolaminated layers with a thickness of 26 nm [65, 66]. The nanolaminated layers were synthesized using

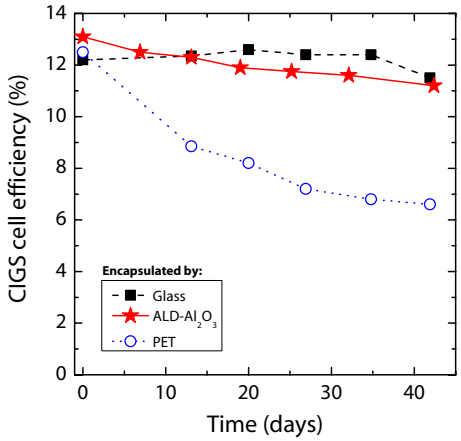


**Figure 6.** Efficiency of CIGS cells encapsulated with an ALD-$Al_2O_3$ layer, a glass lid, and a plastic lid of polyethylene terephthalate (PET). The efficiency was monitored over days, under conditions of 85 °C/85% relative humidity (reprinted from [61], copyright 2010, with permission from Elsevier).

52 'super-cycles', each consisting of two cycles of $Al_2O_3$ and three cycles of $HfO_2$. A water vapour transmission rate of less than 5 × $10^{-4}$ g $m^{-2}$ $day^{-1}$ (65 °C/60% relative humidity), and the fact that the devices were able to maintain over 70% of their initial power conversion efficiency after air storage and accelerated ageing tests, show that the OPV cells were effectively encapsulated [66]. Also in this case, the ALD process at 140 °C served as a beneficial annealing step. The annealing induced aggregation of the two different polymer domains, which facilitates the transport of charge carriers through these domains [65]. It is interesting to highlight that in these cells the ZnO electron selective layer and the 0.6 nm thick $HfO_2$ hole blocking layer were also deposited by ALD [66]. This device configuration had an initial efficiency of 4.5%.

## 5. Barrier layers for dye-sensitized solar cells

Dye-sensitized solar cells (DSSCs) are one of the emerging technologies based on abundant and low-cost materials, and simple processing techniques. One of the limiting factors of DSSCs is the recombination of charge carriers at the interface of the photoanode and the dye or electrolyte. The application of a barrier layer suppresses these recombination processes due to the greater diffusion length of electrons in the photoanode. However, a barrier layer also decreases the charge injection from the dye into the photoanode. Therefore, a trade-off in thickness is required. The capability of ALD to coat high-aspect ratio surfaces with a high quality barrier layer of a few atomic layers thick is exploited for this type of solar cells.

A variety of materials deposited by ALD have been studied as a barrier layer for different photoanode structures (see table 1). For instance, $TiO_2$ nanoparticles coated with thin $Al_2O_3$ layers (using $Al(CH_3)_3$ and $H_2O$) resulted in improved solar cell performances [74–80, 119]. These good results have been related to the high recombination energy barrier of the $Al_2O_3$-$TiO_2$ interface, the high work function of the $Al_2O_3$ barrier layer, and the low energy barrier between the dye and $Al_2O_3$ [78]. The ALD process requires a long soaking

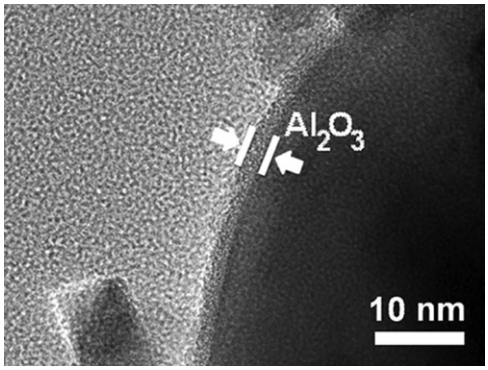


**Figure 7.** High-resolution transmission electron microscope (HR-TEM) image of a DSSC with $TiO_2$ electrode coated with 20 ALD cycles of $Al_2O_3$. (Reproduced from [75] by permission of The Royal Society of Chemistry.)

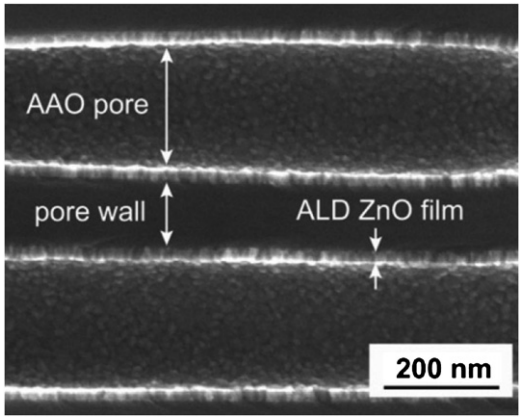


**Figure 8.** Cross-sectional scanning electron microscope (SEM) image of anodic aluminium oxide (AAO) membrane pores coated with 20 nm ALD-ZnO. (Reprinted with permission from [90]. Copyright 2007 American Chemical Society.)

period (∼2 min) after each exposure of the reactants to obtain a conformal coating within the nanoporous structure. A very time-consuming process can however be avoided because it was found that optimal barrier performance can be obtained by depositing only one ALD cycle of $Al_2O_3$ (∼0.1 nm) [74–77, 119]. One such ALD cycle does not fully cover the $TiO_2$ surface, but it is hypothesized that the dye bonds only to the $Al_2O_3$ barrier layer because the contact with the $TiO_2$ is prevented by steric hindrance [75]. However, discrepancies in the thickness values reported in the literature exist on this matter. Several authors reported that thicknesses of ∼2 nm are required [79, 80], but in theory these thicker layers should have a lower performance as a barrier layer since the rate of electron tunnelling from the dye to the $TiO_2$ decays exponentially with the barrier thickness [81]. The HR-TEM image presented in figure 7 shows a $TiO_2$ nanoparticle that was conformally coated with 20 ALD cycles (∼2 nm) [75].

Efficiencies of 6.5% have been reported for DSSCs with $TiO_2$/ALD-$Al_2O_3$ core-shell structures [75, 76], which are similar to that reported for DSSCs with $Al_2O_3$ layers prepared by other methods such as sol-gel coating. The use of ALD presents an advantage because it is not wet chemical while the films can still be deposited at low temperatures. This makes ALD an attractive technique for plastic-based flexible DSSCs.

## 6. ALD for nanostructured solar cells

Besides the application of ALD in well-established solar cell concepts such as c-Si and CIGS solar cells, ALD has also been used to produce nanostructures for emerging solar cell concepts. These concepts are not likely to become economically viable in the near future, however it is still worth briefly addressing them in this review.

ALD can be used to fabricate novel photoanode structures to further improve the performance of DSSCs. Martinson *et al* synthesised high-surface-area ZnO nanotube photoanodes by combining anodic aluminium oxide templating and ALD [90, 120]. As shown in figure 8, the capability of ALD to conformally coat nanometre-sized pores was successfully exploited to obtain oriented arrays of electrically interconnected semiconductor nanotubes. These nanotubes provided direct paths for charge collection over a thickness of tens of micrometres and exhibited therefore much faster transport than nanoparticle networks. Hamann *et al* used low-density, high-surface-area, mesoporous aerogels of silica as a template to fabricate pseudo-one-dimensional $TiO_2$ and ZnO photoanodes [86, 89]. Both $TiO_2$ and ZnO were conformally deposited with controlled variable thicknesses on the aerogel templates by ALD. Power conversion efficiencies of over 5% have been reported for DSSC devices with these nanostructured photoanodes [121].

Goossens and co-workers deposited $Cu_xS$ and $CuInS_2$ films by ALD to be used as absorber materials in nanostructured heterojunction solar cells [95–99]. For these three-dimensional solar cell concepts, $CuInS_2$ was infiltrated by ALD into the pores of nanostructured $TiO_2$. The infiltration process relied again on the excellent conformality that can be obtained by ALD. In addition, buffer layers of $In_2S_3$ and $Al_2O_3$ were deposited in the same ALD reactor as the $CuInS_2$ photoactive material. The application of a stack of 2 nm $Al_2O_3$ and 10 nm $In_2S_3$ between the $TiO_2$ and $CuInS_2$ layers improved the device performance significantly [99]. Efficiencies of 4% were obtained on solar cells of a few square centimetres in area.

## 7. The prospects of ALD in solar cell manufacturing

From the overview of the efforts to apply ALD in various solar cell concepts it is clear that ALD is a technique which is of high interest for the field of photovoltaics. As introduced in the previous sections, ALD has several unique features which can be used to face processing challenges in different types of solar cells. For the application in industrial PV production, however, high-throughput manufacturing is essential. So far, the deposition rates that can be obtained in conventional single wafer reactors (see figure 9(*a*)) as often used in research, are considered too low. Even for the almost 'ideal' ALD process of $Al_2O_3$, the growth rate is not more than a few nm per minute on planar substrates [146]. Fortunately, the growth rate of ALD (nm $min^{-1}$) does not simply relate to the throughput

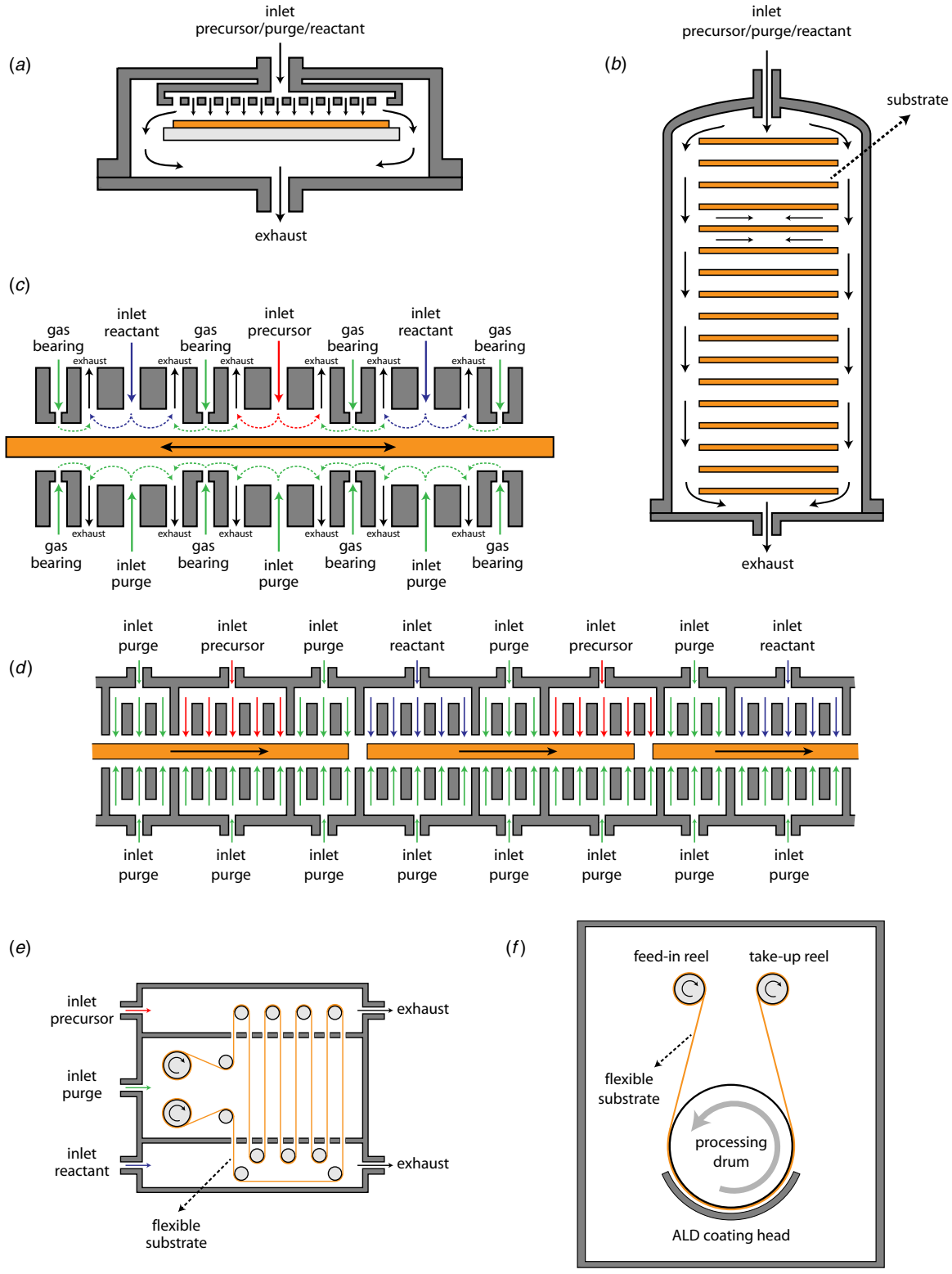


**Figure 9.** Schematic representations of various ALD reactor designs: (*a*) showerhead type single wafer ALD reactor; (*b*) batch ALD reactor [122]; (*c*) in-line spatial ALD reactor as designed by SoLayTec [148, 149]; (*d*) in-line spatial ALD reactor as designed by Levitech [134]; (*e*) roll-to-roll ALD reactor as designed by Lotus Applied Technology [142]; (*f*) roll-to-roll ALD reactor as designed by Beneq [124].

(nm $min^{-1}$ $m^{-2}$) of an ALD system. Scaling up to batch reactors as well as novel ALD reactor designs can increase the throughput drastically. Depending on the type of solar cell, different strategies can be employed, all having their particular strengths and challenges. Critical issues include high-uniformity over large areas and reactant handling and

injection. Achievements and challenges for batch ALD, large-area ALD, spatial and in-line ALD and roll-to-roll ALD are addressed in the following subsections.

### *7.1. Batch ALD*

Batch reactors are one of the earliest high-throughput ALD reactor designs using a single reactor chamber to process multiple substrates (see figure 9(*b*)). Typically, these reactors can process 50–500 substrates in a single deposition run [122, 123]. Scaling up from single wafer reactor to batch reactor is, however, not straightforward. First of all, the reactant exposure and purging times need to be longer than those in single wafer reactors due to the larger reactor volume and lower gas conductance between multiple substrates [3]. Fortunately, the advantage of processing multiple substrates at the same time balance out the longer processing times positively. Secondly, only the more ideal ALD processes are suited for batch operation, unless the conditions are relaxed (e.g. lower demands on uniformity). Finally, single-side deposition can be challenging, for example when surfaces are textured such that the surface texture of the wafers hinders adequate back-to-back wafer stacking. Despite these challenges, ALD batch processing is currently under development by several companies to meet the high quality and throughput demands of the PV industry [124–127]. The Finish company Beneq, for example, is on the verge of commercializing a high-throughput batch reactor (TFS NX300) especially designed for the deposition of $Al_2O_3$ surface passivation layers for c-Si solar cells [124]. It is expected that with this reactor a maximum throughput of 3200 wafers per hour can be obtained for 20 nm thick $Al_2O_3$ films.

### *7.2. Large-area ALD*

The use of large-area substrates is another strategy that contributes to increase the throughput of ALD. Large-area ALD reactors can be single wafer or batch reactors that in both cases share the same benefits and drawbacks as the batch reactors described in the previous subsection. A single wafer type of large-area reactor is developed by Beneq for the deposition of Cd-free buffer layers in CIGS solar cells. The reactor is based on the cross flow ALD concept (i.e. flow of precursors is parallel to the substrate surface), and can deposit $60 \times 120\,cm^2$ CIGS panels with 20 nm Zn(O,S) at a (typically required) throughput of 24 panels per hour [123, 124]. The large-area CIGS panels can be uniformly coated ($\pm 3\%$) with ALD cycle times of only 2 s. The fact that the system meets the very demanding requirements for both thin-film quality and process throughput makes Cd-free ALD buffer layers a true alternative to the conventional CBD-CdS buffer layers.

### *7.3. Spatial and in-line ALD*

A completely different strategy is the so-called spatial ALD concept. In this concept the ALD cycles are carried out in the spatial domain rather than in the time domain. This means that precursor and reactant pulsing occur at different positions using different reaction zones separated by purging areas. Therefore, in order to expose the substrate to these different zones, either the substrate itself or an 'ALD deposition head' must move. The use of purge areas, created by inert gas barriers, requires high pressure operation. In this case, the throughput is merely limited by the technical specifications of the reactor (e.g. substrate loading, reactor size/length, etc.) as well as the speed and kinetics of the surface reactions. For processes with typical half-reaction time scales in the order of a few milliseconds, very high deposition rates can be obtained while maintaining a high film quality.

The basic concept of spatial ALD was already presented by Suntola *et al* in 1983 [128]; however, it was Levi *et al* from the Eastman-Kodak company who really pioneered it experimentally for application in thin-film transistors [129, 130]. The interest in this concept for PV followed after the promising results of $Al_2O_3$ films deposited by ALD to passivate the surface of c-Si solar cells [102, 103]. Two companies, SoLayTec and Levitech [131, 132], are currently developing in-line systems based on the spatial ALD concept, aiming at a throughput of more than 3000 wafers per hour to meet the industrial requirements [133–139]. The main difference between the two designs is the way of transporting the wafers (see figures 9(*c*) and (*d*)). In Levitech's system the wafer is propelled continuously in one direction while the wafer is moved back and forth in SoLayTec's system. Both systems show very promising results in terms of throughput and material quality. A high level of surface passivation, similar to that of $Al_2O_3$ obtained in single wafer reactors, has been obtained in proof-of-principle reactors [133, 134]. The passivation quality of the $Al_2O_3$ films after firing was tested and was well within the specifications for advanced passivation applications [134, 135]. The main benefit of these systems is that they operate under atmospheric pressure and that neither gas switching valves nor vacuum pumps are needed. Furthermore, no deposition occurs at the reactor walls as every part of the reactor is only exposed to one of the reactants at most.

The first successful implementation of spatial ALD of $Al_2O_3$ films into solar cells was reported in 2010 using Levitech's system [16]. The $Al_2O_3$ films were implemented in the ASPIRe (all sides passivated and integrated at the rear) cell concept—a combination of metal wrap through and rear surface passivation technologies—showing initial efficiencies up to 16.6%. Even though Levitech's reactor was still under development at that stage, the achieved efficiencies were very encouraging as they were approximately 1% absolute higher than those for similar cells passivated by *a*-$SiN_x$:H films. Very recently, also the good passivation quality of Levitech's spatial ALD-$Al_2O_3$ films on boron-diffused *p*-type emitters was demonstrated [18]. An efficiency of 18.3% was achieved for *n*-type Si solar cells with an $Al_2O_3$ layer thickness of 5 nm.

### *7.4. Roll-to-roll ALD*

The promising results obtained by the implementation of substrate movement in the ALD process led to new reactor designs for specific applications. The roll-to-roll ALD concept was conceived for coating flexible substrates. This ALD

approach can be exploited to encapsulate flexible PV devices with the industrially required high throughput. Different concepts are being considered to realize roll-to-roll processes [124, 140–142]. All these approaches have in common that the precursor gases are confined in certain volumes, and that the flexible substrate is transferred through these volumes to enable the right exposure of the substrate to the various precursors. Lotus Applied Technology, for instance, reported on a static low pressure deposition chamber where the flexible substrate is passed through a sequence of slit valves from the purge zone to the precursor or reactant zone (see figure 9(*e*)) [142–144]. This setup led to the deposition of high-quality barrier layers on both sides of the substrate with a speed up to 20 m $min^{-1}$ [144]. Beneq reported a roll-to-roll ALD process where the flexible substrate rolls from a feed-in reel through the ALD process section—consisting of a rotating drum and an ALD coating head—and ends at a take-up reel (see figure 9(*f*)) [124]. In a proof-of-concept reactor, the relevant parameters for this roll-to-roll ALD process were studied and showed a good film uniformity across the 300 mm × 100 mm flexible substrate at a temperature of about 100 °C [140, 145]. The new proposed system is capable to coat 500 mm wide flexible substrates with a speed up to 2 m $min^{-1}$ [124].

The above-mentioned efforts represent a first step to establish true industrial roll-to-roll ALD, but further development of these systems will remain necessary. Industrial pilot-scale roll-to-roll ALD systems are expected to be implemented within a 1–2 years time frame [146].

## 8. Conclusions and outlook

Atomic layer deposition has attracted extensive scientific and technological interest in the last decade due to its capability of depositing high-quality thin films with precise growth control, exceptional uniformity, and excellent step coverage on non-planar surfaces. The applications of ALD-prepared thin films in several solar cells concepts discussed in this review clearly illustrate the prospects of ALD to improve solar cell efficiencies. Among all, the application of ALD passivation layers in c-Si solar cells and ALD buffer layers in CIGS solar cells are considered the most promising for the PV industry in the coming years. It is expected that these two applications can compete with established technologies, and therefore have a significant market potential.

The ALD technique has the opportunity to have an even wider scale implementation in the PV industry if a few remaining challenges are addressed. For instance, the high-throughput manufacturing processes developed so far use the more 'ideal' ALD precursors such as $Al(CH_3)_3$ and $Zn(C_2H_5)_2$, which are liquids, highly reactive, and highly volatile. Unfortunately, for some processes only solid and/or low-vapour pressure precursors are available and their use is challenging for deposition over large areas and for processing at atmospheric pressure. Therefore, future research should focus on precursor development to widen the choice of ALD precursors available for high-throughput processing. Other challenges are related to applications using temperature-sensitive materials, such as for example in polymers-based solar cells. The deposition of high quality materials at low temperatures (<100 °C) is quite challenging. This difficulty could be overcome by the use of plasma-assisted ALD processes that allow for deposition at these low temperatures [147].

The state of ALD research for photovoltaic applications puts ALD on the right track to become part of the standard solar cell process equipment in the near future. Despite the conservative production-oriented mindset of the PV industry, it is expected that ALD will be fully embraced at the moment high-throughput ALD equipment achieve better performance with lower costs than existing deposition techniques. Considering the remarkable advances and quick increase in interest in ALD technology in the last few years this moment could be in the near future.

## Acknowledgments

This work was financially supported by the Technology Foundation STW, applied science division of the Netherlands Organization for Scientific Research (VICI-program, 10817). The research of one of the authors (D.G.-A.) has been made possible by a Marie Curie Intra-European Fellowship of the European Community's Seventh Framework Programme (ALD4PV, FP7-MC-IEF-272444).

## References

[1] Ritala M and Leskelä M ed H S Nalwa 2002 *Handbook of Thin Film Materials* (San Diego, CA: Academic Press) pp 103–159
[2] Puurunen R L 2005 *J. Appl. Phys.* **97** 121301
[3] George S M 2010 *Chem. Rev.* **110** 111–31
[4] Hayafuji N, Eldallal G M, Dip A, Colter P C, Elmasry N A and Bedair S M 1994 *Appl. Surf. Sci.* **82-3** 18–22
[5] Eldallal G M, Abou-Elwafa M S, Elgammal M A and Bedair S M 1995 *Renew. Energy* **6** 713–8
[6] Ohtake Y, Kushiya K, Ichikawa M, Yamada A and Konagai M 1995 *Japan. J. Appl. Phys.* **34** 5949–55
[7] Sang B S, Yamada A and Konagai M 1998 *Japan. J. Appl. Phys.* **37** L206–8
[8] Sang B S, Dairiki K, Yamada A and Konagai M 1999 *Japan. J. Appl. Phys.* **38** 4983–8
[9] Bakke J R, Pickrahn K L, Brennan T P and Bent S F 2011 *Nanoscale* **3** 3482–508
[10] Bock R, Schmidt J, Mau S, Hoex B and Brendel R 2010 *IEEE Trans. Electron Devices* **57** 1966–71
[11] Schmidt J, Merkle A, Brendel R, Hoex B, van de Sanden M C M and Kessels W M M 2008 *Prog. Photovolt. Res. Appl.* **16** 461–6
[12] Schmidt J *et al* 2010 *25th European Photovoltaic Solar Energy Conf. and Exhibition (Valencia)*
[13] Saint-Cast P, Benick J, Kania D, Weiss L, Hofmann M, Rentsch J, Preu R and Glunz S W 2010 *IEEE Electron Device Lett.* **31** 695–7
[14] Benick J, Hoex B, van de Sanden M C M, Kessels W M M, Schultz O and Glunz S W 2008 *Appl. Phys. Lett.* **92** 253504
[15] Sun W C, Chang W L, Chen C H, Du C H, Wang T Y, Wang T and Lan C W 2009 *Electrochem. Solid-State Lett.* **12** H388–91
[16] Romijn I G *et al* 2010 *25th European Photovoltaic Solar Energy Conf. and Exhibition (Valencia)*

[17] Ebser J, Junge J, Lüder T, Seren S, Terheiden B and Hahn G 2010 *25th European Photovoltaic Solar Energy Conf. and Exhibition (Valencia)*

[18] Brand P, Veschetti Y, Sanzone V, Cabal R, Pagés X, Vanormelingen K and Vermont P 2011 *37th IEEE Photovoltaic Specialists Conf. (Seattle)*

[19] Vermang B *et al* 2011 *26th European Photovoltaic Solar Energy Conf. and Exhibition (Hamburg)*

[20] Schmidt J, Veith B, Werner F, Zielke D and Brendel R 2010 *35th IEEE Photovoltaic Specialists Conf. (Honolulu)* 885–90

[21] Gatz S, Hannebauer H, Hesse R, Werner F, Schmidt A, Dullweber T, Schmidt J, Bothe K and Brendel R 2011 *Phys. Status Solidi RRL* **5** 147–9

[22] Cruz-Campa J L, Okandan M, Resnick P J, Clews P, Pluym T, Grubbs R K, Gupta V P, Zubia D and Nielson G N 2011 *Sol. Energy Mater. Sol. Cells* **95** 551–8

[23] Richter A, Henneck S, Benick J, Hörteis M, Hermle M and Glunz S W 2010 *25th European Photovoltaic Solar Energy Conf. and Exhibition (Valencia)*

[24] Reichel C, Reusch M, Granek F, Hermle M and Glunz S W 2010 *35th IEEE Photovoltaic Specialists Conf. (Honolulu)* 1034–8

[25] Dullweber T, Gatz S, Hannebauer H, Falcon T, Hesse R, Schmidt J and Brendel R 2011 *Prog. Photovolt. Res. Appl.* early view doi:10.1002/pip.1198

[26] Petermann J H, Zielke D, Schmidt J, Haase F, Rojas E G and Brendel R 2011 *Prog. Photovolt. Res. Appl.* **20** 1–5

[27] Suwito D, Jäger U, Benick J, Janz S, Hermle M and Glunz S W 2010 *IEEE Trans. Electron Devices* **57** 2032–6

[28] Richter A, Benick J, Kalio A, Seiffe J, Hörteis M, Hermle M and Glunz S W 2011 *Energy Procedia* **8** 479–86

[29] Schmiga C, Hermle M and Glunz S W 2008 *23rd European Photovoltaic Solar Energy Conf. and Exhibition (Valencia)*

[30] Kiefer F, Ulzhöfer C, Brendemühl T, Harder N P, Brendel R, Mertens V, Bordihn S, Peters C and Müller J W 2011 *IEEE J. Photovolt.* **1** 49–53

[31] Vanormelingen K, Vermont P and Granneman E H A 2011 *26th European Photovoltaic Solar Energy Conf. and Exhibition (Hamburg)*

[32] Hultqvist A, Platzer-Björkman C, Törndahl T, Ruth M and Edoff M 2007 *22nd European Photovoltaic Solar Energy Conf. and Exhibition (Milan)*

[33] Hultqvist A, Platzer-Björkman C, Pettersson J, Törndahl T and Edoff M 2009 *Thin Solid Films* **517** 2305–8

[34] Platzer-Björkman C, Törndahl T, Hultqvist A, Kessler J and Edoff M 2007 *Thin Solid Films* **515** 6024–7

[35] Platzer-Björkman C, Zabierowski P, Pettersson J, Törndahl T and Edoff M 2010 *Prog. Photovolt. Res. Appl.* **18** 249–56

[36] Törndahl T, Platzer-Björkman C, Kessler J and Edoff M 2007 *Prog. Photovolt. Res. Appl.* **15** 225–35

[37] Törndahl T, Coronel E, Hultqvist A, Platzer-Björkman C, Leifer K and Edoff M 2009 *Prog. Photovolt. Res. Appl.* **17** 115–25

[38] Pettersson J, Platzer-Björkman C and Edoff M 2009 *Prog. Photovolt. Res. Appl.* **17** 460–9

[39] Genevée P, Donsanti F, Renou G and Lincot D 2010 *25th European Photovoltaic Solar Energy Conf. and Exhibition (Valencia)*

[40] Hultqvist A, Platzer-Björkman C, Coronel E and Edoff M 2011 *Sol. Energy Mater. Sol. Cells* **95** 497–503

[41] Platzer-Björkman C, Kessler J and Stolt L 2003 *3rd World Conf. on Photovoltaic Energy Conversion (Osaka)*

[42] Platzer-Björkman C, Törndahl T, Abou-Ras D, Malmström J, Kessler J and Stolt L 2006 *J. Appl. Phys.* **100** 044506

[43] Yousfi E B, Asikainen T, Pietu V, Cowache P, Powalla M and Lincot D 2000 *Thin Solid Films* **361** 183–6

[44] Zimmermann U, Ruth M and Edoff M 2006 *21st European Photovoltaic Solar Energy Conf. and Exhibition (Dresden)*

[45] Abou-Ras D, Rudmann D, Kostorz G, Spiering S, Powalla M and Tiwari A N 2005 *J. Appl. Phys.* **97** 084908

[46] Guillemoles J F *et al* 2001 *Japan. J. Appl. Phys.* **40** 6065–8

[47] Naghavi N, Spiering S, Powalla M, Cavana B and Lincot D 2003 *Prog. Photovolt. Res. Appl.* **11** 437–43

[48] Spiering S, Hariskos D, Powalla M, Naghavi N and Lincot D 2003 *Thin Solid Films* **431** 359–63

[49] Spiering S, Eicke A, Hariskos D, Powalla M, Naghavi N and Lincot D 2004 *Thin Solid Films* **451** 562–6

[50] Spiering S, Hariskos D, Schröder S and Powalla M 2005 *Thin Solid Films* **480** 195–8

[51] Sterner J, Malmström J and Stolt L 2005 *Prog. Photovolt. Res. Appl.* **13** 179–93

[52] Chaisitsak S, Sugiyama T, Yamada A and Konagai M 1999 *Japan. J. Appl. Phys.* **38** 4989–92

[53] Chaisitsak S, Yamada A, Konagai M and Saito K 2000 *Japan. J. Appl. Phys.* **39** 1660–4

[54] Malm U, Malmström J, Platzer-Björkman C and Stolt L 2005 *Thin Solid Films* **480** 208–12

[55] Platzer-Björkman C, Lu J, Kessler J and Stolt L 2003 *Thin Solid Films* **431** 321–5

[56] Shimizu A, Chaisitsak S, Sugiyama T, Yamada A and Konagai M 2000 *Thin Solid Films* **361** 193–7

[57] Hultqvist A, Edoff M and Törndahl T 2011 *Prog. Photovolt. Res. Appl.* **19** 478–81

[58] Hultqvist A, Platzer-Björkman C, Zimmermann U, Edoff M and Törndahl T 2011 *Prog. Photovolt. Res. Appl.* early view doi:10.1002/pip.1153

[59] Bae D, Choi C, Lee J, Kwon S, Lee J, Kim W and Park K 2011 *37th IEEE Photovoltaic Specialists Conf. (Seattle)*

[60] Hegedus S, Carcia P F, McLean R S and Culver B 2010 *35th IEEE Photovoltaic Specialists Conf. (Honolulu)* 1178–83

[61] Carcia P F, McLean R S and Hegedus S 2010 *Sol. Energy Mater. Sol. Cells* **94** 2375–8

[62] Perrenoud J, Buecheler S, Kranz L, Fella C, Skarp J and Tiwari A N 2010 *35th IEEE Photovoltaic Specialists Conf. (Honolulu)* 995–1000

[63] Potscavage W J, Yoo S, Domercq B and Kippelen B 2007 *Appl. Phys. Lett.* **90** 253511

[64] Sarkar S, Culp J H, Whyland J T, Garvan M and Misra V 2010 *Org. Electron.* **11** 1896–900

[65] Chang C Y, Chou C T, Lee Y J, Chen M J and Tsai F Y 2009 *Org. Electron* **10** 1300–6

[66] Chang C Y and Tsai F Y 2011 *J. Mater. Chem.* **21** 5710–5

[67] Zhou Y H, Cheun H, Potscavage W J, Fuentes-Hernandez C, Kim S J and Kippelen B 2010 *J. Mater. Chem.* **20** 6189–94

[68] Wang J C, Weng W T, Tsai M Y, Lee M K, Horng S F, Perng T P, Kei C C, Yu C C and Meng H F 2010 *J. Mater. Chem.* **20** 862–6

[69] Cheun H, Fuentes-Hernandez C, Zhou Y H, Potscavage W J, Kim S J, Shim J, Dindar A and Kippelen B 2010 *J. Phys. Chem.* C **114** 20713–8

[70] Schmidt H, Flügge H, Winkler T, Bülow T, Riedl T and Kowalsky W 2009 *Appl. Phys. Lett.* **94** 243302

[71] Kang Y J, Kim C S, Kwon S H and Kang J W 2011 *37th IEEE Photovoltaic Specialists Conf. (Seattle)*

[72] Saarenpää H, Niemi T, Tukiainen A, Lemmetyinen H and Tkachenko N 2010 *Sol. Energy Mater. Sol. Cells* **94** 1379–83

[73] Law M, Greene L E, Radenovic A, Kuykendall T, Liphardt J and Yang P D 2006 *J. Phys. Chem.* B **110** 22652–63

[74] Hamann T W, Farha O K and Hupp J T 2008 *J. Phys. Chem.* C **112** 19756–64

[75] Lin C, Tsai F Y, Lee M H, Lee C H, Tien T C, Wang L P and Tsai S Y 2009 *J. Mater. Chem.* **19** 2999–3003

[76] Tien T C, Pan F M, Wang L P, Lee C H, Tung Y L, Tsai S Y, Lin C, Tsai F Y and Chen S J 2009 *Nanotechnology* **20** 305201

[77] Klahr B M and Hamann T W 2009 *J. Phys. Chem.* C **113** 14040–5

[78] Tien T C, Pan F M, Wang L P, Tsai F Y and Lin C 2010 *J. Phys. Chem.* C **114** 10048–53

[79] Ganapathy V, Karunagaran B and Rhee S W 2010 *J. Power Sources* **195** 5138–43

[80] Shanmugam M, Baroughi M F and Galipeau D 2010 *Thin Solid Films* **518** 2678–82

[81] Prasittichai C and Hupp J T 2010 *J. Phys. Chem. Lett.* **1** 1611–5

[82] Antila L J *et al* 2011 *J. Phys. Chem.* C **115** 16720–9

[83] Park K, Zhang Q F, Garcia B B, Zhou X Y, Jeong Y H and Cao G Z 2010 *Adv. Mater.* **22** 2329–32

[84] Tétreault N, Arsenault E, Heiniger L P, Soheilnia N, Brillet J, Moehl T, Zakeeruddin S, Ozin G A and Grätzel M 2011 *Nano Lett.* **11** 4579–84

[85] Li T C, Goes M S, Fabregat-Santiago F, Bisquert J, Bueno P R, Prasittichai C, Hupp J T and Marks T J 2009 *J. Phys. Chem.* C **113** 18385–90

[86] Hamann T W, Martinson A B F, Elam J W, Pellin M J and Hupp J T 2008 *J. Phys. Chem.* C **112** 10303–7

[87] Martinson A B F, Elam J W, Liu J, Pellin M J, Marks T J and Hupp J T 2008 *Nano Lett.* **8** 2862–6

[88] Han T H, Moon H S, Hwang J O, Seok S I, Im S H and Kim S O 2010 *Nanotechnology* **21** 185601

[89] Hamann T W, Martinson A B F, Elam J W, Pellin M J and Hupp J T 2008 *Adv. Mater.* **20** 1560–4

[90] Martinson A B F, Elam J W, Hupp J T and Pellin M J 2007 *Nano Lett.* **7** 2183–7

[91] Martinson A B F, Giebink N C, Wiederrecht G P, Rosenmann D and Wasielewski M R 2011 *Energy Environ. Sci.* **4** 2980–5

[92] Choi J W, Kwon S H, Jeong Y K, Kim I and Kim K H 2011 *J. Electrochem. Soc.* **158** B749–53

[93] Bills B, Shanmugam M and Baroughi M F 2011 *Thin Solid Films* **519** 7803–8

[94] Sarkar S K, Kim J Y, Goldstein D N, Neale N R, Zhu K, Elliot C M, Frank A J and George S M 2010 *J. Phys. Chem.* C **114** 8032–9

[95] Reijnen L, Meester B, Goossens A and Schoonman J 2003 *Chem. Vap. Deposition* **9** 15–20

[96] Nanu M, Reijnen L, Meester B, Goossens A and Schoonman J 2003 *Thin Solid Films* **431** 492–6

[97] Nanu M, Schoonman J and Goossens A 2004 *Adv. Mater.* **16** 453–6

[98] Nanu M, Reijnen L, Meester B, Schoonman J and Goossens A 2004 *Chem. Vap. Deposition* **10** 45–9

[99] Nanu M, Schoonman J and Goossens A 2005 *Adv. Funct. Mater.* **15** 95–100

[100] Lenzmann F, Nanu M, Kijatkina O and Belaidi A 2004 *Thin Solid Films* **451** 639–43

[101] Glunz S W *et al* 2005 *20th European Photovoltaic Solar Energy Conf. and Exhibition (Barcelona)*

[102] Hoex B, Heil S B S, Langereis E, van de Sanden M C M and Kessels W M M 2006 *Appl. Phys. Lett.* **89** 042112

[103] Agostinelli G, Delabie A, Vitanov P, Alexieva Z, Dekkers H F W, De Wolf S and Beaucarne G 2006 *Sol. Energy Mater. Sol. Cells* **90** 3438–43

[104] Dingemans G, van de Sanden M C M and Kessels W M M 2010 *Electrochem. Solid-State Lett.* **13** H76–9

[105] Dingemans G, Terlinden N M, Pierreux D, Profijt H B, van de Sanden M C M and Kessels W M M 2011 *Electrochem. Solid-State Lett.* **14** H1–4

[106] Dingemans G, Seguin R, Engelhart P, van de Sanden M C M and Kessels W M M 2010 *Phys. Status Solidi RRL* **4** 10–2

[107] Benick J, Richter A, Hermle M and Glunz S W 2009 *Phys. Status Solidi RRL* **3** 233–5

[108] Dingemans G, Engelhart P, Seguin R, Einsele F, Hoex B, van de Sanden M C M and Kessels W M M 2009 *J. Appl. Phys.* **106** 114907

[109] Dingemans G, van de Sanden M C M and Kessels W M M 2011 *Phys. Status Solidi RRL* **5** 22–4

[110] Schmidt J, Veith B and Brendel R 2009 *Phys. Status Solidi RRL* **3** 287–9

[111] Dingemans G and Kessels W M M 2010 *25th European Photovoltaic Solar Energy Conf. and Exhibition (Valencia)*

[112] Hoex B, Schmidt J, Bock R, Altermatt P P, van de Sanden M C M and Kessels W M M 2007 *Appl. Phys. Lett.* **91** 112107

[113] Hoex B, Schmidt J, Pohl P, van de Sanden M C M and Kessels W M M 2008 *J. Appl. Phys.* **104** 044903

[114] Benick J, Leimenstoll A and Schultz O 2007 *22nd European Photovoltaic Solar Energy Conf. and Exhibition (Milan)*

[115] ScienceLab MSDS for cadmium www.sciencelab.com/msds.php?msdsId=9923223 (last accessed: February 15, 2012)

[116] Naghavi N *et al* 2010 *Prog. Photovolt. Res. Appl.* **18** 411–33

[117] Naghavi N, Renou G, Bockelee V, Donsanti F, Genevée P, Jubault M, Guillemoles J F and Lincot D 2011 *Thin Solid Films* **519** 7600–5

[118] Pettersson J, Platzer-Björkman C, Hultqvist A, Zimmerman U and Edoff M 2010 *Phys. Scr.* **T141** 014010

[119] Antila L J, Heikkila M J, Aumanen V, Kemell M, Myllyperkio P, Leskela M and Korppi-Tommola J E I 2010 *J. Phys. Chem. Lett.* **1** 536–9

[120] Martinson A B F, Goes M S, Fabregat-Santiago F, Bisquert J, Pellin M J and Hupp J T 2009 *J. Phys. Chem.* A **113** 4015–21

[121] Hamann T W, Jensen R A, Martinson A B F, Van Ryswyk H and Hupp J T 2008 *Energy Environ. Sci.* **1** 66–78

[122] Granneman E H A, Fischer P, Pierreux D, Terhorst H and Zagwijn P 2007 *Surf. Coat. Technol.* **201** 8899–907

[123] Skarp J I 2010 *ESC Trans.* **33** 447–52

[124] Beneq http://www.beneq.com (last accessed: February 15, 2012)

[125] ASM http://www.asm.com (last accessed: February 15, 2012)

[126] Picosun http://www.picosun.com (last accessed: February 15, 2012)

[127] NCD Technology http://www.ncdtech.co.kr (last accessed: February 15, 2012)

[128] Suntola T S, Pakkala A J and Lindfors S G 1983 *US Patent* 4413022

[129] Levy D H, Freeman D, Nelson S F, Cowdery-Corvan P J and Irving L M 2008 *Appl. Phys. Lett.* **92** 192101

[130] Levy D H, Nelson S F and Freeman D 2009 *J. Disp. Technol.* **5** 484–94

[131] SoLayTec http://solaytec.org (last accessed: February 15, 2012)

[132] Levitech http://www.levitech.nl (last accessed: February 15, 2012)

[133] Poodt P, Lankhorst A, Roozeboom F, Spee K, Maas D and Vermeer A 2010 *Adv. Mater.* **22** 3564–7

[134] Granneman E H A, Vermont P, Kuznetsov V I, Coolen M and Vanormelingen K 2010 *25th European Photovoltaic Solar Energy Conf. and Exhibition 2010 Valencia*

[135] Vermang B, Rothschild A, Racz A, John J, Poortmans J, Mertens R, Poodt P, Tiba V and Roozeboom F 2011 *Prog. Photovolt. Res. Appl.* **19** 733–9

[136] Poodt P, Kniknie B, Branca A, Winands H and Roozeboom F 2011 *Phys. Status Solidi RRL* **5** 165–7

[137] Kuznetsov V I, Granneman E H A, Vermont P and Vanormelingen K 2010 *ESC Trans.* **33** 441–6

[138] Poodt P, Tiba V, Werner F, Schmidt J, Vermeer A and Roozeboom F 2011 *J. Electrochem. Soc* **158** H937–40
[139] Vermont P, Kuznetsov V I and Granneman E H A 2011 *26th European Photovoltaic Solar Energy Conf. and Exhibition (Hamburg)*
[140] Maydannik P S, Kääriäinen T O and Cameron D C 2011 *Chem. Eng. J.* **171** 345–9
[141] Poodt P, Knaapen R, Illiberi A, Roozeboom F and van Asten A 2012 *J. Vac. Sci. Technol.* A **30** 01A142–5
[142] Dickey E R and Barrow W A 2009 *52th Annual Technical Conf. Proc. on the Society of Vacuum Coaters (Santa Clara)* 720–6
[143] Lotus Applied Technology http://www.lotusat.com (last accessed: February 15, 2012)
[144] Dickey E R 2011 *11th Int. Conf. on Atomic Layer Deposition (Cambridge)*
[145] Lahtinen K, Maydannik P S, Johansson P, Kääriäinen T O, Cameron D C and Kuusipalo J 2011 *Surf. Coat. Technol.* **205** 3916–22
[146] Kessels W M M and Putkonen M 2011 *MRS Bull.* **36** 907–13
[147] Profijt H B, Potts S E, van de Sanden M C M and Kessels W M M 2011 *J. Vac. Sci. Technol.* A **29** 050801
[148] Vermeer A, Roozeboom F, Poodt P and Görtzen R 2011 *MRS Proc.* **1323** c04-04
[149] Poodt P, Cameron D C, Dickey E, George S M, Kuznetsov V, Parsons G N, Roozeboom F, Sundaram G and Vermeer A 2012 *J. Vac. Sci. Technol.* **30** 010802